International Journal of Environment and Health Sciences (IJEHS)
2024, VOL. 6, NO. 4, 59-64
https://doi.org/10.47062/1190.0601.02

GREEN SYNTHESIS, CHARACTERIZATION OF CUO AND RGO/CUO NANOCOMPOSITES VIA REFLUX METHOD

Roopa M C[1], Sharadadevi Kallimani[1] and Thirumala S[2]*

[1]Department of Studies in Environmental Science
Davangere University, Davangere - 577004, Karnataka, India.
[2]Department of Environmental Science,
Government First Grade College Harihara – 577601, Karnataka, India.

Received on: 10.08.2024 **Revised on:** 22.09.2024 **Accepted on:** 07.10.2024

Abstract
This study focuses on the green synthesis of CuO and rGO/CuO via the reflux technique. The produced materials can be confirmed by conducting various analytical techniques. The analysis revealed particle sizes of approximately 29.35 nm for CuO and 23.56 nm for rGO/CuO. Internal and surface morphology studies confirmed the well-developed particles formed on rGO sheets. UV-Vis's analysis provided absorbance data and band gap values, while elemental analysis confirmed the presence of copper, oxygen, and carbon. FT-IR spectra identified metal-oxygen bonds within the 600-400 cm ^{1} range in both CuO and rGO/CuO. These materials demonstrate broad potential applications, including photocatalysis, antioxidant and antifungal activities, sewage and industrial dye water treatment, energy storage, and corrosion resistance.

Keywords: rGO; CuO; Green synthesis; Reflux method; Characterization.

1. INTRODUCTION

In ancient Egypt, from 2000 BCE, copper was employed for water purification and sterilization. Additionally, it was used for treating wounds, showcasing its significant role in early medical practices. The antibacterial properties of copper have been recognized for centuries. During the Roman Empire, copper was commonly used in cooking pots, which inadvertently helped reduce bacterial contamination in food and water. Copper's ability to kill bacteria and other microorganisms stems from its oligodynamic effect, where even small amounts of copper ions disrupt essential microbial processes, leading to cell death. This ancient application highlights an early, albeit indirect, understanding of copper's antimicrobial properties. Copper was also employed to prevent the spread of communicable diseases. Notably, Japanese soldiers placed small pieces of copper in their water flasks throughout the Second World War to avoid dysentery [1].

However, copper ions can raise concerns about their impact on workers, organizations, and ecosystems [2]. In this context, several studies have explored copper-based nanomaterials as reservoirs for controlled ion release, aiming to mitigate the continuous discharge of Cu^{+} in the nature [3]. CuO exhibit a oxidation rate than their bulk counterparts when exposed to air due to both physic and chemical instability [4]. CuO are constant, highly durable, a extended shelf life equated to other materials or chemical compounds [5]. However, as soon as nanomaterials are reintroduced to interest in biological media, they tend to convert unbalanced, foremost to the increased combination of antibacterial agents and a subsequent reduction in their effectiveness. In this context, a practical solution is incorporating them into films or supportive matrices, enhancing their stability and effectiveness [6]. For instance, an appropriate material is graphene, which is only one atom thick, solid, and flat, consisting of sp^{2}-bonded carbon atoms in a hexagonal 2D lattice [7]. In the most informed approaches for synthesizing CuO/graphene nanocomposites, copper salts are introduced into ethanol-covering exfoliated graphene. Following synthesis, the resulting nanoparticles typically range from 25 to 200 nm [8]. Recently, CuO/graphene nanocomposites have

CONTACT *Corresponding author: *drst2008@gmail.com*
Color versions of one or more of the figures in this article can be found online at www.stenvironment.org

been synthesized through a straightforward method involving mixing graphene with CuO nanoparticles by a usual size of approximately 60 nm [9]. Graphene oxide (GO) stands out as an oxidized graphene derivative among the various graphene-related compounds. Graphene oxide offers a large surface area, the potential to incorporate numerous initiated functional groups, respectable water dispersion, and a moderately simple research process. Its biocompatibility further enhances its suitability as a support material, making it an excellent platform for nanomaterials [10]. This material enhances the constancy of nanoparticles and improves their antibacterial performance, which is attributed to the formation of ultrafine particles.

Additionally, GO can boost the adsorption assets for Cu (II) ions, exhibiting a high adsorption capacity for copper ions. Studies show that graphene oxide can improve the adsorption capacity by approximately 30% [11]. Cu salts are precursors, along with an aqueous graphene oxide (GO) dispersion in an alkaline solution. The mixture is then reduced, assisted by oxidation in the presence of a complexing agent, using methods such as microwave irradiation, NaOH, or heat [12]. In these studies, the size of CuO nanoparticles ranged from 30 to 400 nm [13]. Therefore, a reduction in the size of nanomaterials can significantly enhance their efficiency and performance [14-15]

The current investigation is a modest green synthesis scheme for CuO and a reflux method for synthesizing rGO/CuO nanocomposites. The materials have been categorized us ing several practices, such as XRD, SEM, EDAX, FTIR, UV-Vis, and HRTEM analysis. The prepared materials include tenders in catalysis, photodegradation, microbial activity, antifungal treatments, and anticancer therapies.

2. MATERIAL SYNTHESIS

2.1. Preparation of CuO using Ashwagandha plant fuel

A silica crucible was used to dissolve 1 g of $Cu(NO_3)_2$ in a very minimal of water. Half a gram of dried Ashwagandha herb was used as fuel. The mixture was kept in furnace at 600°C for one hour under oxygen-rich open combustion conditions. The corresponding reaction equation is shown below (Eq. 1) [16].

$$Cu(NO_3)_2 * 3H_2O + \text{Ashwagandha (fuel)} \rightarrow CuO + CO_2(g) + H_2O \ldots\ldots (1)$$

2.2. Synthesis of rGO/CuO via reflux method

0.1 g of rGO was sonicated for 30 minutes and added to an RB flask. Separately, 0.25 g of CuO was mixed with 30 mL of water in the RB flask. The combination was stirred magnetically at 400 rpm and heated to 90°C for 30 minutes. Subsequently, 1% sodium sulfite and 1 g of sodium citrate were added to the reaction mixture and stirred for one hour. Finally, 2 M NaOH was added into the mixture, which was stirred for 30 mins. The solution was then allowed to settle for a few minutes, passed through Whatman filter paper, and dried for 30 minutes at 60°C in the oven [17].

3. RESULTS DISCUSSION

3.1. XRD

The XRD of CuO and rGO/CuO are presented in Fig. 1. CuO was synthesized using the SCM. The diffraction peaks observed at 31.59°, 36.75°, 38.32°, 48.78°, 52.56°, 58.21°, 60.27°, 65.43°, 68.34°, 72.34°, and 75.34° resemble the Miller planes (110), (11-1), (111), (20-2), (020), (202), (11-3), (31-1), (220), (311), and (22-2), respectively. These peaks line up well with the usual JCPDS card number 48–1548, confirming the formation of CuO [18]. In the XRD of rGO/CuO, a prominent peak observed at 24°-25° agrees with the (002) plane of rGO, indicating its successful incorporation into the composite. This high-intensity peak confirms the presence of rGO alongside CuO, synthesized by the reflux method. The remaining peaks correspond to CuO, with no additional peaks observed, thereby confirming the purity of the composite material and the absence of impurities [19]. The size was determined using the Eq. (2),

$$D = \frac{K\lambda}{\beta Cos\theta} \ldots\ldots (2)$$

For CuO, the size was found to be 29.35 nm, whereas for rGO/CuO, it was 23.56 nm.

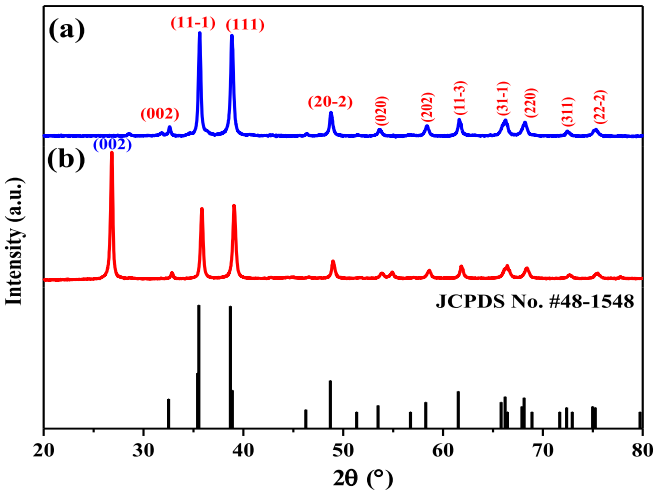

Figure 1. (a, b) XRD of CuO and rGO/CuO.

3.2. SEM and TEM

The SEM image of CuO and rGO/CuO was displayed in Fig. 2(a, b). In Fig. 2(a), the SEM of CuO particles exhibits an even distribution throughout the whole surface area of a spherical form. Additionally, nearly vacant spaces are observed within the compound, which could be attributed to the synthesis process [20]. Fig. 2(b) illustrates an SEM image of rGO/CuO, where the graphene sheet matrix is uniformly decorated with CuO particles. The surface morphology analysis further approves the practical synthesis of the rGO/CuO, as such uniform dispersion indicates the effective integration of CuO onto the graphene layers. In Fig. 2(c), the internal reveals well-defined spherical particles distributed across the surface of the rGO sheets. The CuO are closely packed and clustered, indicating strong interaction and integration with the rGO matrix [21].

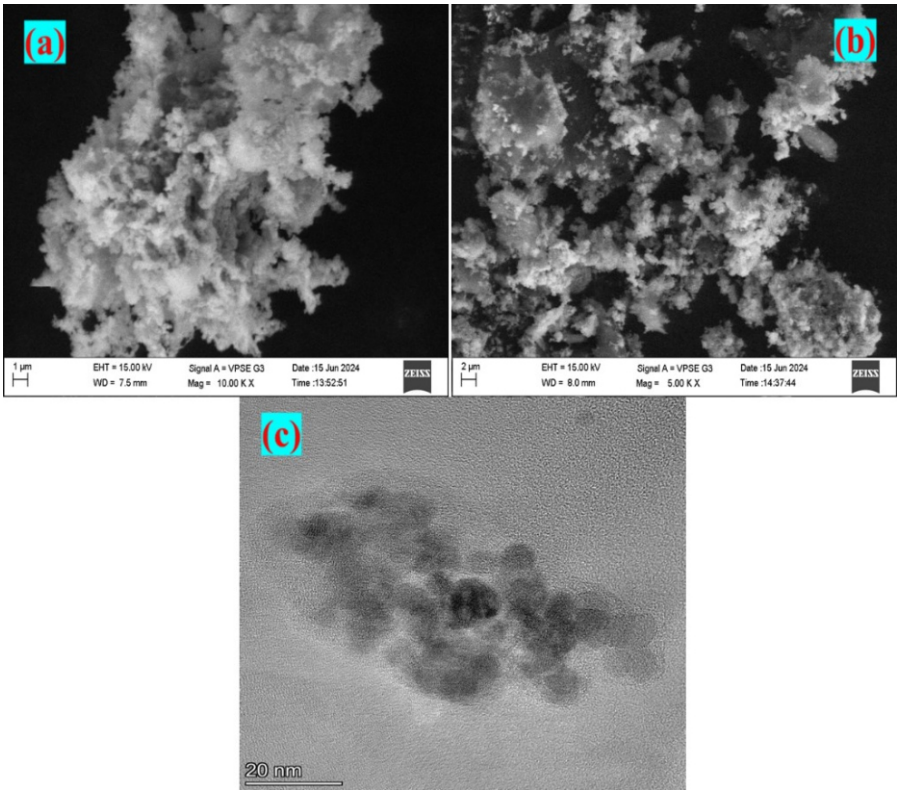

Figure 2. SEM of (a, b) CuO, rGO/CuO and (c) TEM of rGO/CuO.

3.3. EDX

EDX analysis of the synthesized rGO/CuO composite, in Fig. 3, displays prominent peaks for Cu, C, and O, confirming the production of rGO/CuO via the reflux technique. The absence of any additional peaks in the spectrum indicates the composite's purity and validates the synthesis process's effectiveness [22].

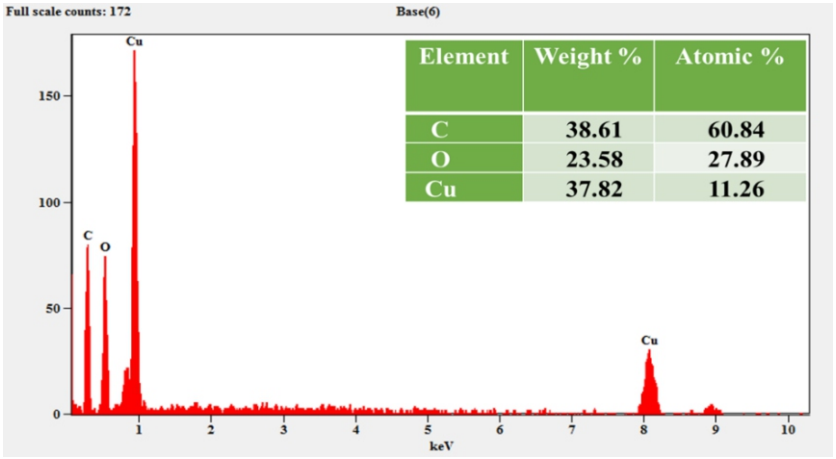

Figure 3. EDX image of rGO/CuO.

3.4. UV-Vis spectroscopy and Bandgap

The UV studies and band gap analysis in Fig. 4. The absorption spectra confirmed the Energy band gap using the Kubelka Munk curve under Eq. (3) [44].

$$\mathbf{F(R)} = \frac{\mathbf{(1-R^2)}}{\mathbf{2R}} \ldots\ldots\ldots\ldots\ldots \mathbf{(3)}$$

$$(\boldsymbol{F(R)hV})^2 = \boldsymbol{C}\left(\boldsymbol{hV} - \boldsymbol{E_g}\right) \ldots\ldots\ldots\ldots\ldots \mathbf{(4)}$$

The plot of (F(R)hν)2 vs photon energy (hν) and the energy band gap Eg are shown in Fig. 4. According to Eq (4), the expression (F(R)hν)2 is used to determine the optical band gap. From the band gap values shown in Fig. 4(a, b) (inset), it has been noted that the CuO and rGO/CuO have band gaps of 4.78 and 1.43 eV [23].

3.5. FTIR

The C-O vibrations are responsible for the peak at 1117 cm¹ in the rGO/CuO seen in Fig. 5. The peak shows the existence of

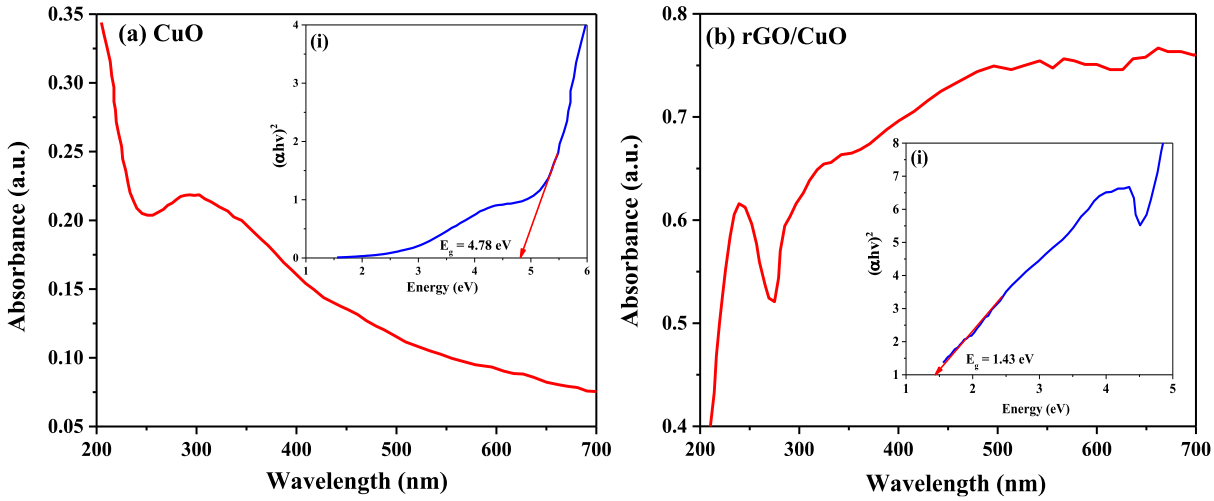

Figure 4: (a, b) UV-Vis and (inset) Tauc's plot of CuO and rGO/CuO.

C-C bonds inside the GO sheets at 1566 cm $^{-1}$. O–H vibrations are observed around 3389 cm $^{-1}$, though weak in the rGO [24]. The peak at 882 cm $^{-1}$ is attributed to Cu-OH bond vibrations, further confirmatory the successful synthesis of rGO/CuO. The absence of CuO-specific peaks and a peak at 432 cm $^{-1}$, corresponding to Cu-O, validate that CuO has been effectively into the rGO sheets [25].

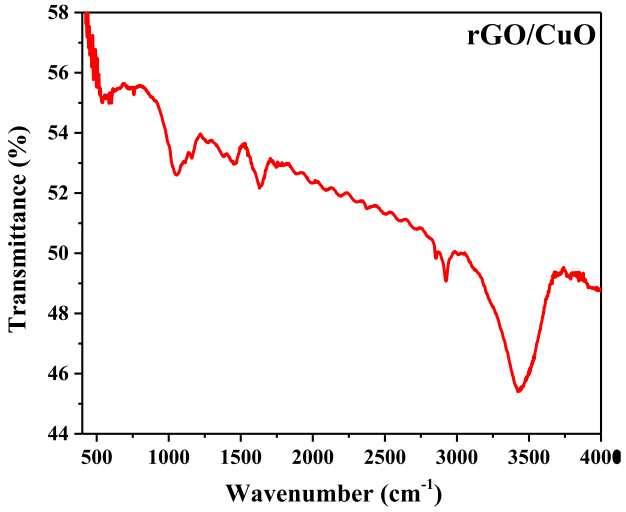

Figure 5 IR of rGO/CuO.

4.CONCLUSION

The green approach of CuO and rGO/CuO by means of the reflux method has proven to be a practical approach for producing nanomaterials with promising applications in various fields. The characterization results confirm the successful synthesis of well-defined CuO and rGO/CuO particles with optimal sizes and surface morphologies. These materials exhibit an extensive choice of potential uses, particularly in photocatalysis, environmental remediation, sensor, and corrosion resistance. Future work will optimize the synthesis process and explore their execution for practical purposes, such as wastewater treatment and energy devices, to maximize their impact on sustainable technologies.

REFERENCES

1. **L. Tamayo, M. Azócar, M. Kogan, A. Riveros, M. Páez**, Copper-polymer nanocomposites: An excellent and cost-effective biocide for use on antibacterial surfaces, Materials Science and Engineering: C 69 (2016) 1391–1409. https://doi.org/10.1016/j.msec.2016.08.041.

2. **J.H. Chen, H.T. Xing, X. Sun, Z.B. Su, Y.H. Huang, W. Weng, S.R. Hu, H.X. Guo, W.B. Wu, Y.S. He,** Highly effective removal of Cu(II) by triethylenetetramine-magnetic reduced graphene oxide composite, *Applied Surface Science*. 356 (2015) 355–363. https://doi.org/10.1016/j.apsusc.2015.08.076.

3. **M. Valodkar, P.S. Rathore, R.N. Jadeja, M. Thounaojam, R.V. Devkar, S. Thakore**. Cytotoxicity evaluation and antimicrobial studies of starch capped water soluble copper nanoparticles, Journal of Hazardous Materials 201–202 (2012) 244–249. https://doi.org/10.1016/j.jhazmat.2011.11.077.

4. **B. Li, Y. Li, Y. Wu, Y. Zhao**. Synthesis of water-soluble Cu/PAA composite flowers and their antibacterial activities. *Materials Science and Engineering*: C 35 (2014) 205–211. https://doi.org/10.1016/j.msec.2013.11.006.

5. **D. Das, B.C. Nath, P. Phukon, S.K. Dolui**, Synthesis and evaluation of antioxidant and antibacterial behavior of CuO nanoparticles, Colloids and Surfaces B: Biointerfaces. 101 (2013) 430–433. https://doi.org/10.1016/j.colsurfb.2012.07.002.

6. **B. Marta, M. Potara, M. Iliut, E. Jakab, T. Radu, F. Imre-Lucaci, G. Katona, O. Popescu, S. Astilean**. Designing chitosan–silver nanoparticles–graphene oxide nanohybrids with enhanced antibacterial activity against Staphylococcus aureus, Colloids and Surfaces A: Physicochemical and Engineering Aspects 487 (2015) 113–120. https://doi.org/10.1016/j.colsurfa.2015.09.046.

7. **C. Qin, J. Fei, P. Cai, J. Zhao, J. Li**. Biomimetic membrane-conjugated graphene nanoarchitecture for light-manipulating combined cancer treatment *in vitro*, *Journal of Colloid and Interface Science*. 482 (2016) 121–130. https://doi.org/10.1016/j.jcis.2016.07.031.
8. **B. Wang, X.-L. Wu, C.-Y. Shu, Y.-G. Guo, C.-R. Wang.** Synthesis of CuO/graphene nanocomposite as a high-performance anode material for lithium-ion batteries. *J. Mater. Chem*. 20 (2010) 10661. https://doi.org/10.1039/c0jm01941k.
9. ,**V. Sharma, S.M. Mobin**. Cytocompatible peroxidase mimic CuO:graphene nanosphere composite as colorimetric dual sensor for hydrogen peroxide and cholesterol with its logic gate implementation, Sensors and Actuators B: Chemical. 240 (2017) 338–348. https://doi.org/10.1016/j.snb.2016.08.169.
10. **S. Pourbeyram**. Effective Removal of Heavy Metals from Aqueous Solutions by Graphene Oxide–Zirconium Phosphate (GO–Zr-P) Nanocomposite, *Ind. Eng. Chem. Res.* 55 (2016) 5608–5617. https://doi.org/10.1021/acs.iecr.6b00728.
11. **S. T. Yang, Y. Chang, H. Wang, G. Liu, S. Chen, Y. Wang, Y. Liu, A. Cao**. Folding/aggregation of graphene oxide and its application in Cu2+ removal. *Journal of Colloid and Interface Science*. 351 (2010) 122–127. https://doi.org/10.1016/j.jcis.2010.07.042.
12. **C. Sarkar, S.K. Dolui**. Synthesis of copper oxide/reduced graphene oxide nanocomposite and its enhanced catalytic activity towards reduction of 4-nitrophenol, RSC Adv. 5 (2015) 60763–60769. https://doi.org/10.1039/C5RA10551J.
13. **X. Zhang, Y. Hu, D. Zhu, A. Xie, Y. Shen**. A novel porous CuO nanorod/rGO composite as a high stability anode material for lithium-ion batteries. *Ceramics International*. 42 (2016) 1833–1839. https://doi.org/10.1016/j.ceramint.2015.09.147.
14. **P. Kalimuthu, S.A. John**. Size dependent electrocatalytic activity of gold nanoparticles immobilized onto three dimensional sol–gel network, *Journal of Electroanalytical Chemistry*. 617 (2008) 164–170. https://doi.org/10.1016/j.jelechem.2008.02.012.
15. **M. Valodkar, A. Bhadoria, J. Pohnerkar, M. Mohan, S. Thakore**. Morphology and antibacterial activity of carbohydrate-stabilized silver nanoparticles, *Carbohydrate Research*. 345 (2010) 1767–1773. https://doi.org/10.1016/j.carres.2010.05.005.
16. **M.C. Roopa, S. Thirumala, S. Kallimani, B.M. Manohara**. Green and Reflux method synthesis of CeO2/rGO for their characterization and Photodegradation of dye, Sustainable Chemistry One World 4 (2024) 100024. https://doi.org/10.1016/j.scowo.2024.100024.
17. **M.C. Roopa, S. Thirumala, S. Kallimani, B.M. Manohara**. Green synthesis and characterization of nano reduced graphene oxide/cerium oxide (rGO/CeO2) for Rose Bengal dye degradation. *Journal of Alloys and Compounds Communications*. 4 (2024) 100033. https://doi.org/10.1016/j.jacomc.2024.100033.
18. **D. Zhang, N. Yin, C. Jiang, B. Xia**. Characterization of CuO–reduced graphene oxide sandwiched nanostructure and its hydrogen sensing characteristics. *J Mater Sci: Mater Electron*. 28 (2017) 2763–2768. https://doi.org/10.1007/s10854-016-5856-8.
19. **S. Pourbeyram, R. Bayrami, H. Dadkhah**. Green synthesis and characterization of ultrafine copper oxide reduced graphene oxide (CuO/rGO) nanocomposite, Colloids and Surfaces A: Physicochemical and Engineering Aspects 529 (2017) 73–79. https://doi.org/10.1016/j.colsurfa.2017.05.077.
20. **S. Jabeen, V.U. Siddiqui, S. Rastogi, S. Srivastava, S. Bala, N. Ahmad, T. Khan**, Fabrication of B–CuO nanostructure and B-CuO/rGO binary nanocomposite: A comparative study in the context of photodegradation and antimicrobial activity assessment, Materials Today Chemistry 33 (2023) 101712. https://doi.org/10.1016/j.mtchem.2023.101712.
21. **R. Eivazzadeh-Keihan, R. Taheri-Ledari, M.S. Mehrabad, S. Dalvand, H. Sohrabi, A. Maleki, S.M. Mousavi-Khoshdel, A.E. Shalan**. Effective Combination of rGO and CuO Nanomaterials through Poly(*p* -phenylenediamine) Texture: Utilizing It as an Excellent Supercapacitor, Energy Fuels 35 (2021) 10869–10877. https://doi.org/10.1021/acs.energyfuels.1c01132.
22. **S. Sagadevan, Z. Zaman Chowdhury, Mohd.R.B. Johan, F.A. Aziz, E.M. Salleh, A. Hawa, R.F. Rafique**. A one-step facile route synthesis of copper oxide/reduced graphene oxide nanocomposite for supercapacitor applications. *Journal of Experimental Nanoscience*. 13 (2018) 284–296. https://doi.org/10.1080/17458080.2018.1542512.
23. **S. Sagadevan, J.A. Lett, G.K. Weldegebrieal, S. Garg, W.-C. Oh, N.A. Hamizi, M.R. Johan**. Enhanced Photocatalytic Activity of rGO-CuO Nanocomposites for the Degradation of Organic Pollutants, Catalysts 11 (2021) 1008. https://doi.org/10.3390/catal11081008.
24. **M.M. El-Masry**, Synthesize and characterization of Ag-CuO/rGO nanoparticles as a filler of the PVDF polymer to improve its polar β phase and electrical conductivity for polymer batteries applications, *J Polym Res*. 30 (2023) 345. https://doi.org/10.1007/s10965-023-03727-1.
25. **R. Kota, J. Prathipati, M.S. Lakshmi, Y.V. Bhaskara Lakshmi, N. Tamminana**, THE SYNTHESIS OF A COPPER (II) OXIDE (CuO)/ REDUCED GRAPHENE

OXIDE (RGO) NANOCOMPOSITE USING A HYDROTHERMAL METHOD FOR USE IN BIOLOGICAL APPLICATIONS, RJC 17 (2024) 1146–1153. https://doi.org/10.31788/RJC.2024.1738865